

# QCS-ADME: Quantum Circuit Search for Drug Property Prediction with Imbalanced Data and Regression Adaptation

Kangyu Zheng  
zhengk5@rpi.edu

Rensselaer Polytechnic Institute  
Troy, New York, USA

Tianfan Fu  
futianfan@gmail.com

Rensselaer Polytechnic Institute  
Troy, New York, USA

Zhiding Liang  
liangz9@rpi.edu

Rensselaer Polytechnic Institute  
Troy, New York, USA

## Abstract

The biomedical field is beginning to explore the use of quantum machine learning (QML) for tasks traditionally handled by classical machine learning, especially in predicting ADME (absorption, distribution, metabolism, and excretion) properties, which are essential in drug evaluation. However, ADME tasks pose unique challenges for existing quantum computing systems (QCS) frameworks, as they involve both classification with unbalanced dataset and regression problems. These dual requirements make it necessary to adapt and refine current QCS frameworks to effectively address the complexities of ADME predictions.

We propose a novel training-free scoring mechanism to evaluate QML circuit performance on imbalanced classification and regression tasks. Our mechanism demonstrates significant correlation between scoring metrics and test performance on imbalanced classification tasks. Additionally, we develop methods to quantify continuous similarity relationships between quantum states, enabling performance prediction for regression tasks. This represents the first comprehensive approach to searching and evaluating QCS circuits specifically for regression applications.

Validation on representative ADME tasks—one imbalanced classification and one regression—demonstrates moderate positive correlation between our scoring metrics and circuit performance, significantly outperforming baseline scoring methods that show negligible correlation.

## CCS Concepts

• **Computer systems organization** → **Quantum computing**; • **Applied computing** → *Life and medical sciences*; • **Computing methodologies** → *Machine learning*.

## Keywords

Quantum computing, Quantum Circuit Search, Drug property prediction

## ACM Reference Format:

Kangyu Zheng, Tianfan Fu, and Zhiding Liang. 2025. QCS-ADME: Quantum Circuit Search for Drug Property Prediction with Imbalanced Data and

Regression Adaptation. In *Proceedings of Make sure to enter the correct conference title from your rights confirmation email (Conference acronym 'XX)*. ACM, New York, NY, USA, 5 pages. <https://doi.org/XXXXXXXX.XXXXXXX>

## 1 Introduction

Quantum Machine Learning (QML) has gained significant attention for its potential applications on Noisy Intermediate-Scale Quantum (NISQ) hardware [9], demonstrating promising results across various domains [4, 6, 11, 5, 8]. QML architectures differ fundamentally from classical machine learning models in their use of data embedding gates, where gate selection and placement significantly impact performance, and in their gradient computation methods, which employ techniques like parameter-shift rules [10] rather than traditional backpropagation. These unique characteristics make manual circuit design particularly challenging, often resulting in suboptimal performance.

To address this challenge, **Quantum Circuit Search (QCS)** [16, 14, 2] has emerged as a methodology for discovering high-performance, noise-robust circuits, drawing inspiration from classical Neural Architecture Search (NAS) [7]. State-of-the-art QCS approaches [14, 1] generate circuit candidates by employing diverse algorithmic designs and evaluating performance metrics, taking into account hardware specifications and constraints.

The biomedical field has begun exploring QML applications for tasks traditionally addressed by classical machine learning, particularly in ADME (absorption, distribution, metabolism, and excretion) property prediction—crucial characteristics in drug evaluation. However, ADME tasks present unique challenges for existing QCS frameworks, as they encompass both classification and regression problems. Current QCS methods, even the Elivagar [1], a specialized QCS method designed for QML tasks, designed primarily for classification tasks on balanced datasets like MNIST, are not directly applicable to ADME's frequently imbalanced datasets and regression requirements.

To address these limitations, we propose two key methodological enhancements: a weighted matrix approach for unbalanced classification tasks that amplifies minority class representation, and a modified representational capacity score for continuous similarity comparison in regression tasks. We validate these improvements on representative ADME tasks—one unbalanced classification problem and one regression problem—demonstrating improved correlation between our enhanced scoring methods and test performance compared to traditional approaches.

In summary, our contributions are:

1. We propose the first application of the Quantum Circuit Synthesis (QCS) framework to generate quantum machine learning (QML)

Permission to make digital or hard copies of all or part of this work for personal or classroom use is granted without fee provided that copies are not made or distributed for profit or commercial advantage and that copies bear this notice and the full citation on the first page. Copyrights for components of this work owned by others than the author(s) must be honored. Abstracting with credit is permitted. To copy otherwise, or republish, to post on servers or to redistribute to lists, requires prior specific permission and/or a fee. Request permissions from [permissions@acm.org](mailto:permissions@acm.org).

Conference acronym 'XX, Woodstock, NY

© 2025 Copyright held by the owner/author(s). Publication rights licensed to ACM.

ACM ISBN 978-1-4503-XXXX-X/2018/06

<https://doi.org/XXXXXXXX.XXXXXXX>

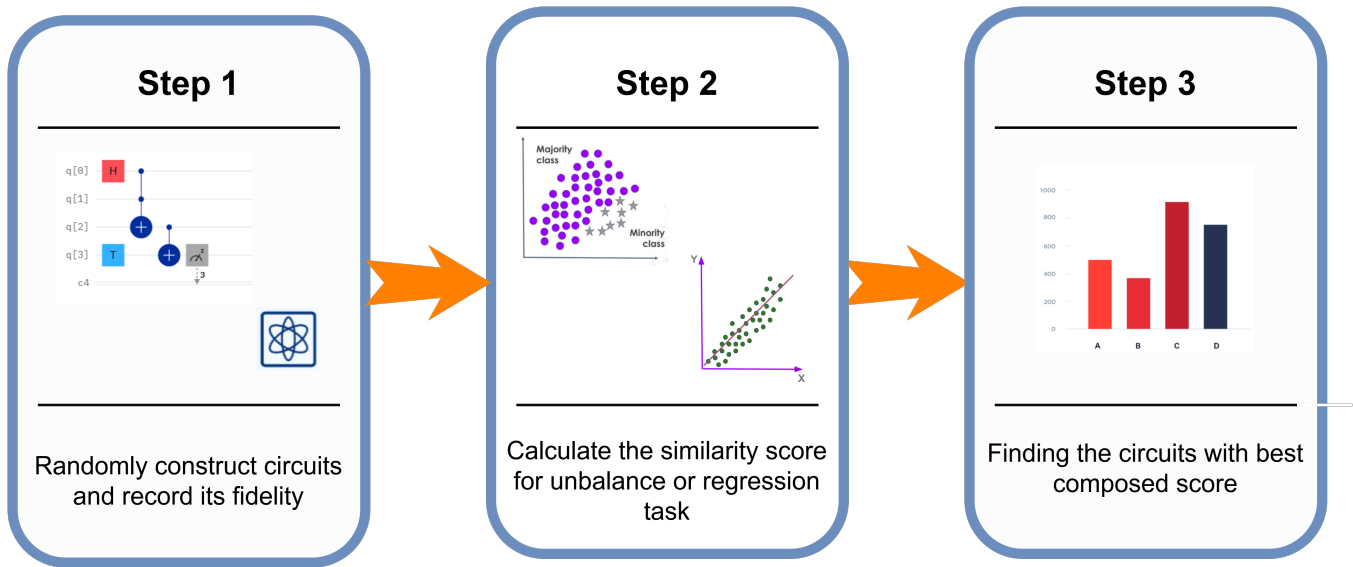


Figure 1: Overview of QCS-ADME

circuits for biomedical ADME tasks (Absorption, Distribution, Metabolism, Excretion).

2. We introduce a novel scoring mechanism for the QCS framework to evaluate circuit performance on imbalanced classification and regression tasks, addressing key challenges in biomedical data analysis.

3. We demonstrate that QML circuits achieve competitive advantages over classical models in specific scenarios (e.g., lower mean squared error in regression tasks) and identify actionable pathways to further improve their robustness for ADME applications.

## 2 Method

To address the requirements of ADME Property Prediction, which encompasses both regression tasks and classification tasks with imbalanced datasets, we enhanced the QCS framework mainly in two key aspects: circuit performance evaluation on imbalanced datasets and regression task handling. Specifically, we chose the Elivagar [1], a state-of-the-art system originally designed for searching QML circuits in balanced binary classification tasks, as our baseline model to improve. This section first outlines Elivagar’s original circuit scoring methodology, followed by our proposed improved structure to accommodate imbalanced classification and regression tasks.

### 2.1 Overview of Elivagar Scoring

Elivagar’s circuit evaluation process consists of two main stages: circuit generation and scoring. Initially, the system generates candidate circuits based on device topology and noise-related parameters. Each candidate circuit is then evaluated using two predictive metrics: Clifford Noise Resilience (CNR) and Representational Capacity (RepCap). CNR predicts circuit fidelity based on structural characteristics, while RepCap quantifies the discriminative power of the circuit by measuring both intra-class similarities and inter-class separation in the final quantum states. These scores are combined

to produce a final metric, where higher values indicate greater potential for superior performance.

The original RepCap scoring mechanism assumes balanced class distributions, as it requires sufficient samples to effectively distinguish between classes. To enable the capability of imbalanced classification and regression tasks common in ADME property prediction, we introduced two key steps: a weighted matrix to account for class imbalance and a revised RepCap calculation methodology for regression tasks.

### 2.2 Handling Class Imbalance

The RepCap metric evaluates circuit performance by measuring class separation in the final quantum state. A circuit receives a higher RepCap score when it maximizes inter-class separation while minimizing intra-class distances. The original RepCap formulation is defined as:

$$\text{RepCap}(C) = 1 - \frac{\|R_C - R_{ref}\|_2^2}{2 \cdot n_c \cdot d_c^2} \quad (1)$$

Here,  $d_c$  denotes the number of samples and  $n_c$  represents the number of classes.  $R_{ref}$  is a  $d \times d$  reference matrix representing ideal circuit predictions, where  $R_{ref}(i, j) = 1$  if samples  $i$  and  $j$  belong to the same class ( $y_i = y_j$ ) and 0 otherwise. The matrix  $R_C$  is also of dimension  $d \times d$  and quantifies the similarity between quantum states of data points  $i$  and  $j$ . While this formulation performs effectively on balanced datasets, it exhibits limitations when handling imbalanced class distributions. In balanced scenarios, the reference matrix contains equal representation for each class. However, when certain classes have significantly more samples than others, the RepCap metric may assign high scores to circuits that excel at distinguishing majority classes while performing poorly on minority classes. To address this limitation, we incorporate classical imbalanced classification techniques by introducing a weight matrix to

the reference matrix, thereby amplifying the importance of minority classes. This modification ensures that circuits must develop robust representations for all classes, regardless of their distribution in the training data, to achieve high scores. The enhanced RepCap formulation is:

$$\text{RepCap}(C) = 1 - \frac{\|R_c - R_w \otimes R_{ref}\|_2^2}{2 \cdot n_c \cdot d_c^2}, \quad (2)$$

where  $R_w$  represents the weight matrix derived from the class distribution in the training data, and  $\otimes$  denotes the element-wise multiplication operation.

### 2.3 Regression Task Adaptation

For regression tasks, we maintain the fundamental structure of the classification approach while introducing key modifications to handle continuous outputs. The first significant modification involves constructing a continuous reference matrix using a Gaussian similarity function to quantify the relationship between target values:

$$R_{ref} = \exp\left(-\frac{\|y_i - y_j\|_2^2}{2\sigma^2}\right), \quad (3)$$

where  $\|y_i - y_j\|_2^2$  represents the squared Euclidean distance between target values, and  $\sigma$  serves as a bandwidth parameter controlling the decay rate of similarity with respect to distance.

The second fundamental modification addresses the quantum state similarity computation. While retaining the basic quantum state similarity calculation framework, we incorporate continuous weighting based on target values. This adaptation is essential because conventional quantum state similarity measurements only capture state relationships in Hilbert space, without considering the proximity of corresponding target values. By introducing target value-dependent Gaussian weighting factors, we ensure the quantum circuit learns to map inputs with similar target values to correspondingly similar quantum states.

These adaptations enable our modified RepCap metric to effectively evaluate circuit performance on regression tasks, providing a more accurate assessment of each candidate circuit’s capabilities. The resulting score more precisely reflects the circuit’s ability to maintain the continuous relationships inherent in regression problems while preserving the quantum state fidelity considerations of the original framework.

## 3 Experiments

### 3.1 Dataset Selection and Preprocessing

From the TDC [13] ADME group, we selected two representative tasks: Cell Effective Permeability (Caco2) [15] for regression and Parallel Artificial Membrane Permeability Assay (PAMPA) [12] for binary classification. The Caco2 dataset requires predicting cell effective permeability values from drug SMILES strings. The PAMPA dataset involves classifying compounds as either high permeability (1) or low-to-moderate permeability (0) based on their SMILES strings. Notably, the PAMPA dataset exhibits significant class imbalance, with a ratio of approximately 6:1 between high and low permeability samples.

To prepare these datasets for our QML circuits, we implemented several preprocessing steps. First, we transformed the SMILES strings

into Molecular ACCESS Systems keys fingerprints (MACCS) [3]. MACCS fingerprints are 166-bit strings where each bit indicates the presence (1) or absence (0) of specific molecular structural features. We utilized the first 128 bits to accommodate our quantum system’s requirements. For the classification task, we remapped all 0 labels to -1. For the regression task, we normalized the target values in both training and testing sets to the range [-1, 1].

### 3.2 Training and Evaluation Configuration

Our training configuration largely follows the Elivagar framework, with necessary adaptations for our specific tasks. We utilized the IBM Rensselaer quantum device architecture and its corresponding noise model for candidate circuit generation. To accommodate our 128-length input features, we configured the system with 7 qubits and employed 32 Clifford replicas for CNR computation. We generated 250 candidate circuits, which were utilized across both classification and regression tasks.

For both tasks, we trained the circuits for 200 epochs with a batch size of 256, using the Adam optimizer with a learning rate of 0.01. The training objective was to minimize the loss between circuit predictions and the corresponding labels or target values in the training set. All training procedures were executed on noiseless simulators using the TorchQuantum [14] framework, with computations performed on a 16-core AMD Ryzen Threadripper PRO 5955WX processor.

In evaluation, we run all the circuits once for both tasks and calculate the final score with the same equation as used by Elivagar.

$$\text{Score}(C) = \text{CNR}(C)^{\alpha_{\text{CNR}}} \times \text{RepCap}(C), \quad (4)$$

where we choose  $\alpha_{\text{CNR}} = 0.25$ .

## 4 Results

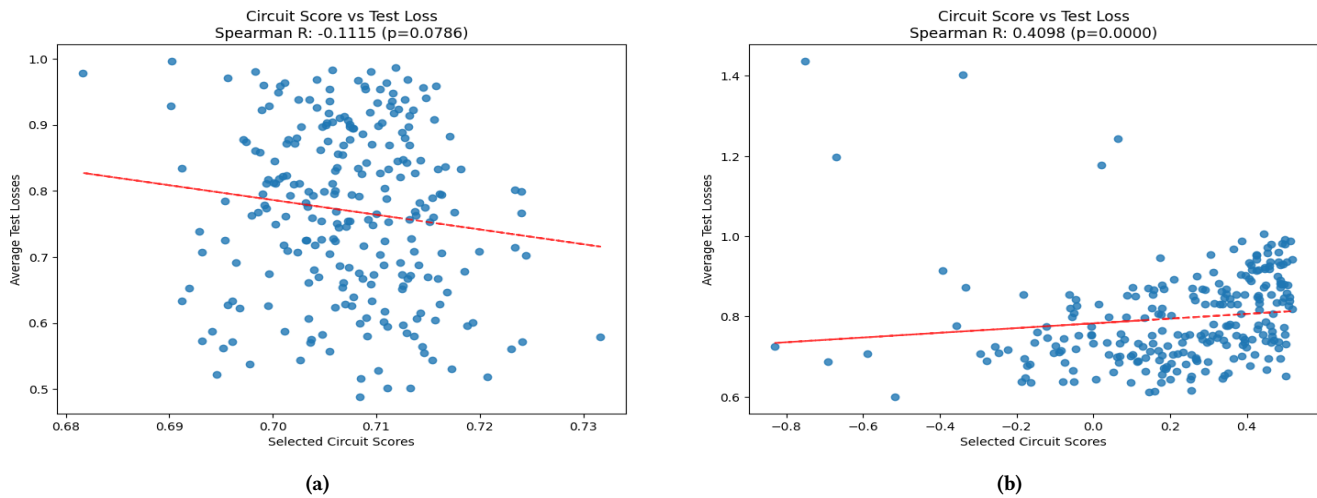
**Table 1: Average and standard deviation of selected metrics for PAMPA test set. The baseline for PRAUC is 0.808.**

Metric	QML average	QML best	XGBoost
MSE	0.7955 ± 0.1195	0.6002	0.1293 ± 0.0134
Accuracy	0.7563 ± 0.0878	0.8250	0.8452 ± 0.0178
F1	0.8507 ± 0.0928	0.8966	0.9116 ± 0.0108
PRAUC	0.8362 ± 0.0368	0.8801	0.9171 ± 0.0170

Metric	Random Forest	SVM
MSE	0.1201 ± 0.0112	0.1111 ± 0.0109
Accuracy	0.8381 ± 0.0180	0.8569 ± 0.0164
F1	0.9101 ± 0.0108	0.9276 ± 0.0094
PRAUC	0.9218 ± 0.0167	0.9195 ± 0.0178

We evaluated our system’s performance using two primary metrics: the Spearman correlation between the final score and test MSE loss, and task-specific performance measures. For the classification task, we analyzed the Spearman correlation between the final score and PR-AUC, while for the regression task, we examined the Spearman correlation between the final score and the Spearman’s rank correlation coefficient of predictions versus true values. These



**Figure 2: Unbalance classification results. (a): Spearman correlation between original final score and test loss of Elivagar [1]. (b): Spearman correlation between revised final score and test loss.**

ranking correlations are particularly crucial in ADME regression tasks.

#### 4.1 Performance on Imbalanced Classification

Figure 2 compares the performance of the original Elivagar scoring system with our enhanced scoring method on the imbalanced classification task. As shown in Figure 2a, the original Elivagar [1] final score demonstrates a weak Spearman correlation (approximately -0.1) with the average test loss, indicating no significant predictive relationship between the scoring metric and actual circuit performance in imbalanced scenarios. In contrast, our revised scoring method achieves a moderate positive Spearman correlation of approximately 0.4 with the test loss, suggesting that our modifications successfully capture circuit performance characteristics in imbalanced classification tasks.

We also evaluate the performance of our quantum-generated circuits against classical machine learning models (XGBoost, Random Forest, SVM) on the PAMPA test set. As shown in Table 1, the QML circuits exhibit a consistent performance gap compared to classical baselines. For example, the best-performing QML circuit achieves an F1-score of 0.8966 and a PRAUC of 0.8801, while classical models such as XGBoost and SVM achieve superior results (F1: 0.9116–0.9276, PRAUC: 0.9171–0.9218). Notably, the average QML performance (e.g., MSE:  $0.7955 \pm 0.1195$  vs. XGBoost:  $0.1293 \pm 0.0134$ ) further underscores this gap. These results highlight the need for improved circuit generation strategies in our QCS framework, particularly to bridge the disparity in robustness and predictive power.

#### 4.2 Regression Task Performance

Figure 3 illustrates our regression task results. Figure 3a shows the correlation between the revised final score and test loss, with a Spearman correlation coefficient of 0.18, indicating a weak positive correlation. Circuits with scores above 0.60 demonstrate consistently higher test losses. However, for circuits with scores below

**Table 2: Average and standard deviation of selected metrics for CaCo2 test set.**

Metric	QML average	QML best	XGBoost
MSE	$0.1376 \pm 0.0336$	0.0955	$0.2421 \pm 0.0242$
Spearman R	$0.0929 \pm 0.1386$	0.4537	$0.7433 \pm 0.0359$

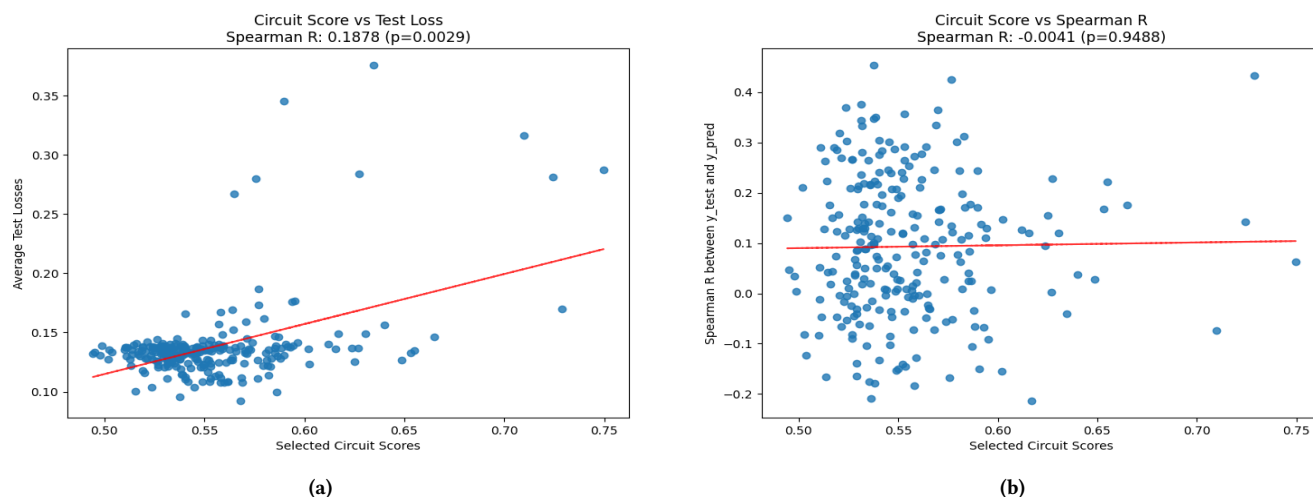
  

Metric	Random Forest	SVR
MSE	$0.1977 \pm 0.0177$	$0.3458 \pm 0.0282$
Spearman R	$0.7321 \pm 0.0361$	$0.5606 \pm 0.0564$

0.6, the test loss clusters between 0.10 and 0.15, indicating limited discriminative power in this range.

We further analyzed the Spearman correlation between circuit predictions and ground truth values on the test set and the result is shown on figure 3b and table 2, as ranking accuracy is particularly relevant for medical applications. The near-zero correlation suggests that while our revised scoring method can identify poorly performing circuits, it has limited ability to predict how well a circuit will model the underlying distribution of the test set.

Finally, we evaluate the regression performance of our generated QML circuits against classical machine learning models (XGBoost, Random Forest, and SVR). As shown in Table 2, the QML circuits demonstrate superior performance, with the best-performing circuit achieving an MSE of 0.0955. This outperforms all classical baselines, including XGBoost ( $0.2421 \pm 0.0242$ ), Random Forest ( $0.1977 \pm 0.0177$ ), and SVR ( $0.3458 \pm 0.0282$ ). Even the average QML performance ( $0.1376 \pm 0.0336$ ) surpasses classical models, highlighting the robustness of our approach. These results underscore the potential of quantum-generated circuits in regression tasks and validate the effectiveness of the circuit generation strategy in our QCS framework.



**Figure 3: Regression results. (a): Spearman correlation between revised score and test loss of Elivagar [1]. (b): Spearman correlation between ranking relation of predicted and ground truth and revised score.**

## 5 Conclusion

This paper presents a QCS framework adapted for unbalanced classification and regression tasks in QML circuits. Building upon an established balanced classification QCS framework, we modified the circuit performance scoring methodology through two key innovations: a weight adjustment matrix for unbalanced tasks and a Gaussian similarity metric for continuous regression relationships. Evaluation on medical task datasets demonstrates moderate correlation between our revised scoring method and final test loss. However, in regression tasks, while our approach successfully identifies low-performance circuits, it shows limitations in predicting circuits' ability to correctly rank test set drugs—a crucial factor for medical applications. This limitation may stem from the disconnect between similarity-based scoring and distribution modeling capability.

Future work will focus on expanding validation across diverse ADME datasets and testing on physical quantum hardware. Additionally, we plan to develop alternative scoring mechanisms specifically tailored for regression tasks.

## References

- [1] Sashwat Anagolum, Narges Alavisamani, Poulami Das, Moinuddin Qureshi, and Yunong Shi. 2024. Elivagar: efficient quantum circuit search for classification. In *Proceedings of the 29th ACM International Conference on Architectural Support for Programming Languages and Operating Systems, Volume 2 (ASPLOS '24)*. Association for Computing Machinery, La Jolla, CA, USA, 336–353. ISBN: 9798400703850. doi:10.1145/3620665.3640354.
- [2] Yuxuan Du, Tao Huang, Shan You, Min-Hsiu Hsieh, and Dacheng Tao. 2022. Quantum circuit architecture search for variational quantum algorithms. *npj Quantum Information*, 8, 1, (May 2022). doi:10.1038/s41534-022-00570-y.
- [3] Joseph L. Durant, Burton A. Leland, Douglas R. Henry, and James G. Nourse. 2002. Reoptimization of mdl keys for use in drug discovery. *Journal of Chemical Information and Computer Sciences*, 42, 6, 1273–1280. PMID: 12444722. eprint: <https://doi.org/10.1021/ci010132r>. doi:10.1021/ci010132r.
- [4] Hsin-Yuan Huang, Michael Broughton, Masoud Mohseni, Ryan Babbush, Sergio Boixo, Hartmut Neven, and Jarrod R. McClean. 2021. Power of data in quantum machine learning. *Nature Communications*, 12, 1, (May 2021). doi:10.1038/s41467-021-22539-9.
- [5] Hsin-Yuan Huang et al. 2022. Quantum advantage in learning from experiments. *Science*, 376, 6598, (June 2022), 1182–1186. doi:10.1126/science.abn7293.
- [6] He-Liang Huang et al. 2021. Experimental quantum generative adversarial networks for image generation. *Physical Review Applied*, 16, 2, (Aug. 2021). doi:10.1103/physrevapplied.16.024051.
- [7] Liam Li and Ameet Talwalkar. 2019. Random search and reproducibility for neural architecture search. (2019). <https://arxiv.org/abs/1902.07638> arXiv: 1902.07638 [cs.LG].
- [8] Yunchao Liu, Srinivasan Arunachalam, and Kristan Temme. 2021. A rigorous and robust quantum speed-up in supervised machine learning. *Nature Physics*, 17, 9, (July 2021), 1013–1017. doi:10.1038/s41567-021-01287-z.
- [9] John Preskill. 2018. Quantum computing in the nisq era and beyond. *Quantum*, 2, (Aug. 2018), 79. doi:10.22331/q-2018-08-06-79.
- [10] Maria Schuld, Ville Bergholm, Christian Gogolin, Josh Izaac, and Nathan Killoran. 2019. Evaluating analytic gradients on quantum hardware. *Physical Review A*, 99, 3, (Mar. 2019). doi:10.1103/physreva.99.032331.
- [11] Daniel Silver, Tirthak Patel, William Cutler, Aditya Ranjan, Harshitta Gandhi, and Devesh Tiwari. 2023. Mosaic: quantum generative adversarial networks for image generation on nisq computers. (2023). <https://arxiv.org/abs/2308.11096> arXiv: 2308.11096 [quant-ph].
- [12] Vishal Siramshetty, Jordan Williams, Dac-Trung Nguyen, Jorge Neyra, Noel Southall, Ewy Mathé, Xin Xu, and Pranav Shah. 2021. Validating adme qsar models using marketed drugs. *SLAS DISCOVERY: Advancing the Science of Drug Discovery*, 26, 10, 1326–1336. PMID: 34176369. eprint: <https://doi.org/10.1177/2472552211017520>. doi:10.1177/2472552211017520.
- [13] Alejandro Velez-Arce, Xiang Lin, Kexin Huang, Michelle M Li, Wenhao Gao, Bradley Pentelute, Tianfan Fu, Manolis Kellis, and Marinka Zitnik. 2024. Signals in the cells: multimodal and contextualized machine learning foundations for therapeutics. In *NeurIPS 2024 Workshop on AI for New Drug Modalities*. <https://openreview.net/forum?id=kL8dlYp6IM>.
- [14] Hanrui Wang, Yongshan Ding, Jiaqi Gu, Yujun Lin, David Z. Pan, Frederic T. Chong, and Song Han. 2022. Quantumnas: noise-adaptive search for robust quantum circuits. In *2022 IEEE International Symposium on High-Performance Computer Architecture (HPCA)*. IEEE, (Apr. 2022), 692–708. doi:10.1109/hpca53966.2022.00057.
- [15] Ning-Ning Wang, Jie Dong, Yin-Hua Deng, Min-Feng Zhu, Ming Wen, Zhi-Jiang Yao, Ai-Ping Lu, Jian-Bing Wang, and Dong-Sheng Cao. 2016. Adme properties evaluation in drug discovery: prediction of Caco-2 cell permeability using a combination of NSGA-II and boosting. *Journal of Chemical Information and Modeling*, 56, 4, (Apr. 2016), 763–773. doi:10.1021/acs.jcim.5b00642.
- [16] Shi-Xin Zhang, Chang-Yu Hsieh, Shengyu Zhang, and Hong Yao. 2022. Differentiable quantum architecture search. *Quantum Science and Technology*, 7, 4, (Aug. 2022), 045023. doi:10.1088/2058-9565/ac87cd.